Electronic Supporting Information

The p-sc structure in Phosphorus: bringing order to the high pressure phases of group 15 elements.

Demetrio Scelta,[†,‡] Adhara Baldassarre,[‡,¶] Manuel Serrano-Ruiz,[†] Kamil Dziubek,[‡] Andrew B. Cairns,[§] Maurizio Peruzzini,[†] Roberto Bini,[‡,¶,†] and Matteo Ceppatelli[*,†,‡]

†*ICCOM-CNR, Institute of Chemistry of OrganoMetallic Compounds, National Research Council of Italy, Via Madonna del Piano 10, I-50019 Sesto Fiorentino, Firenze, Italy*

‡*LENS, European Laboratory for Non-linear Spectroscopy, Via N. Carrara 1, I-50019 Sesto Fiorentino, Firenze, Italy*

¶*Dipartimento di Chimica "Ugo Schiff" dell'Università degli Studi di Firenze, Via della Lastruccia 3, I-50019 Sesto Fiorentino, Firenze, Italy*

§*ESRF, European Synchrotron Radiation Facility, 71 Avenue des Martyrs, 38000 Grenoble, France*

E-mail: ceppa@lens.unifi.it,matteo.ceppatelli@iccom.cnr.it

ESI-1. Phosphorene.

The recent synthesis of Phosphorene,[1,2] a 2D corrugated monoatomic layer of P atoms, has dramatically raised the attention of the scientific community for the layered phases of Phosphorus. The 2D arrangement of the atoms in Phosphorene is indeed structurally related to the semiconducting orthorhombic A17 structure of Phosphorus (Black Phosphorus, *Cmce*, Z=8),[3,4] actually consisting in the ordered stacking of Phosphorene layers, and currently representing the starting material for its synthesis by exfoliation techniques. While chemists, physicists and materials scientists are still facing the challenges set by the synthesis, stabilization and functionalization of Phosphorene and related materials, other 2D Phosphorus allotropes with intriguing properties have been predicted to be stable, stimulating new theoretical and experimental investigations.[5–8]

Experimentally, besides A17, which is the thermodynamically stable allotrope of the element at ambient conditions, at least another layered structure of P can be accessed under high pressure conditions. At room T and ∼4.8 GPa A17 transforms indeed to semimetallic rhombohedral A7 ($R\bar{3}m$, Z=2), another layered structure[9–11] which can be described by the stacking of blue Phosphorene layers[5] and is observed at ambient conditions also in As, Sb and Bi.[12]

ESI-2. Phase diagram of Phosphorus

Above 103 GPa an incommensurate structure (P-IV, IM, *Cmmm(00γ)s00*)[13] has been reported to exist up to 137 GPa, where a conversion to a simple-hexagonal structure (P-V, sh, *P6/mmm*, Z=1), observed up to 282 GPa, has been found to occur.[14–16] A body centered cubic structure (*bcc*),[17,18] successively identified as a superlattice structure (P-VI, *cI16(I$\bar{4}$3d)*), has been then reported to form above 262 GPa and to be stable up to 340 GPa.[19]

ESI-3. The two-step mechanism for the A7 to sc phase transition.

From a crystallographic point of view, assuming a rhombohedral cell description, the existence of the p-sc structure is evinced from the pressure evolution of the A7 lattice parameters. Whereas above 10.5 GPa the angle α rapidly approaches the $\sim$60° limit value characteristic of the sc structure, at $\sim$30 GPa the atomic position u is still far from the 0.250 value expected in the sc structure, thus causing a lattice distortion.[20] With increasing pressure, the electrostatic contribution is expected to become dominant, favoring the achievement of an octahedral coordination and hence the formation of a sc structure.

The observation of the p-sc structure has been interpreted in terms of the strong *s-p* orbital mixing existing in P, which at low pressure is responsible for the presence of electron lone pairs and tetrahedral geometry at P sites.[20]

Moreover, the identification of the key role played by the *s-p* orbital mixing in the persistence of the layers against the interlayer bond formation has provided a fundamental physico-chemical insight for the stabilization of the high pressure layered structures against their reversible transformations upon releasing pressure, thus opening new perspectives for designing and synthesizing Phosphorene-based materials and heterostructures.

ESI-4. Experimental Methods

Room temperature compression and decompression of bP in the presence of different pressure transmitting media (He, H_2, N_2, Daphne 7474 Oil), was studied using DAC and synchrotron XRD under different compression conditions, ranging from nearly hydrostatic to non-hydrostatic. Pressure was generated by means of membrane Diamond Anvil Cells (DAC) equipped with Ia/IIa type standard cut 16-sided beveled anvils having 350/400 μm culet tips. Re gaskets (200 μm) indented to about 70 μm and laser-drilled to obtain a 150 μm diameter hole were used for the sideways containment of the samples. The diffusion of He and H_2 through the gasket at high pressure was prevented by applying a gold ring to the gasket hole. In these cases a larger 200 μm hole was prepared by laser drilling. The gasket was then filled by gold particles, compressed to compact to gold powder and again drilled to obtain a 150 μm hole in the gold. The gold ring surrounding the sample thus prevented any contact of He and H_2 with Re.

The highly crystalline and pure orthorhombic bP used for the experiments was synthesized from red Phosphorus according to reference 21. The reagents used for the synthesis of black phosphorus were purchased from Sigma-Aldrich and their purity was: red phosphorus ($>$ 99.99%), tin ($>$ 99.999%), gold ($>$ 99.99%), and SnI_4 (99.999%). The purity of the synthesized bP crystals used in the experiments reported in this study was verified by X-ray powder diffraction, Raman spectroscopy, EDX analysis and ICP-MS measurements, the latter giving a purity of 99.999+%. The obtained bP crystals were then fragmented and cut by a metallic tip to obtain smaller 20-50 μm chips, which were placed in the sample chamber of the DAC, together with a ruby for the measurement of pressure by the ruby fluorescence method. The DAC was then gas-loaded with high purity (5.0) He and H_2, whereas N_2 was cryo-loaded. In the case of Daphne Oil 7474, a small drop was deposited inside the gasket hole. The use of He allowed to preserve hydrostatic conditions within the investigated pressure range, as indicated by the peak widths.

The samples were studied by means of synchrotron X-ray diffraction (XRD). Due to the

heterogeneity of the sample a micron-sized beam spot diameter of the synchrotron source was used to select different areas of the sample and spot differently oriented bP crystallites to find the reflections necessary for the calculation of the lattice parameters and the unit cell volume. The XRD patterns were acquired at ESRF-ID27 high pressure dedicated beam line using a monochromatic radiation (0.3738 Å wavelength) with beam spot size diameter of 5 μm and a MAR CCD165 detector. Typical acquisition time was 20 s with $\pm$10 degree maximum oscillation. The detector tilt and sample to detector distance were calibrated by CeO_2 standard. The raw images were processed using DIOPTAS software.[22] In the case of He, Rietveld fit of the integrated patterns above 6 GPa to evaluate the lattice parameters, atomic positions and nearest neighbor distances was performed using GSAS-II software.[23] In the case of the other pressure transmitting media, geometrical formulas relating the d-spacing to the lattice parameters through the Miller indexes of the corresponding crystal structures were used to build systems of equations and calculate the lattice parameters values. In this case the d-spacing values were obtained by fitting the peak positions of the XRD patterns with Voigt line shapes after baseline subtraction. Fityk software was used for this purpose.[24]

ESI-5. Rietveld refinement of the XRD data for the A7 and p-sc structures of P in He.

Traditionally, literature has described the A7 structure in terms of hexagonal symmetry with two axial lattice parameters (a and c) and the sc structure in terms of a cubic cell with one axial lattice parameter (a). Our data for the A7 and p-sc structures obtained by Rietveld refinement are instead derived by adopting a rhombohedral cell description with only one axial lattice parameter (respectively a^r_{A7} and a^r_{p-sc}). For comparison purposes, also the axial lattice parameters obtained from our d-spacing data adopting a cell description consistent with previous literature were calculated and reported in Figure S-1. Whereas this procedure is correct in the case of the A7 structure, because the hexagonal and rhombohedral cell descriptions are equivalent, the use of the d-spacing to evaluate a_{sc} from the sc geometric relations is formally wrong, because the p-sc and sc structure are not equivalent. As a matter of fact, this procedure does not take into account the slight lattice distortion of the p-sc compared to sc one (see Figure 4 in ref.[20]) and neglects the presence of the extra peaks in the p-sc structure.

In agreement with previous studies, our data indicate a larger decrease with pressure of the interlayer distances both in the A17 and A7 structure, directly related respectively to the b_{A17} and c_{A7} lattice parameters. The persistence of the A17 peaks even after the appearance of the A7 ones also agrees with literature, where a sluggish transformation is reported for this phase transition.[11]

In the A17 structure a slightly larger compressibility of the Phosphorene layers along the c axis direction with respect to the perpendicular a axis one is also appreciable, confirming the reported anisotropy in the properties of this 2D material. Interestingly, this is the direction along which the electron lone pairs, originating from the s-p orbital mixing, point against each other. Their perturbation is responsible for the A17 to A7 phase transition, where interlayer bond breaking and reconstruction occurs with electron lone pair redistribution, leading to

layers of different conformation for a more efficient packing, as described in the mechanism proposed by Boulfelfel and coauthors.[25] Also in the A7 structure the electron lone pairs point to the interlayer spacing and are thus preferentially perturbed with increasing pressure, as indicated by the pressure evolution of the c_{A7} lattice parameter, which corresponds to the direction perpendicular to the layers and parallel to the electron lone pairs.

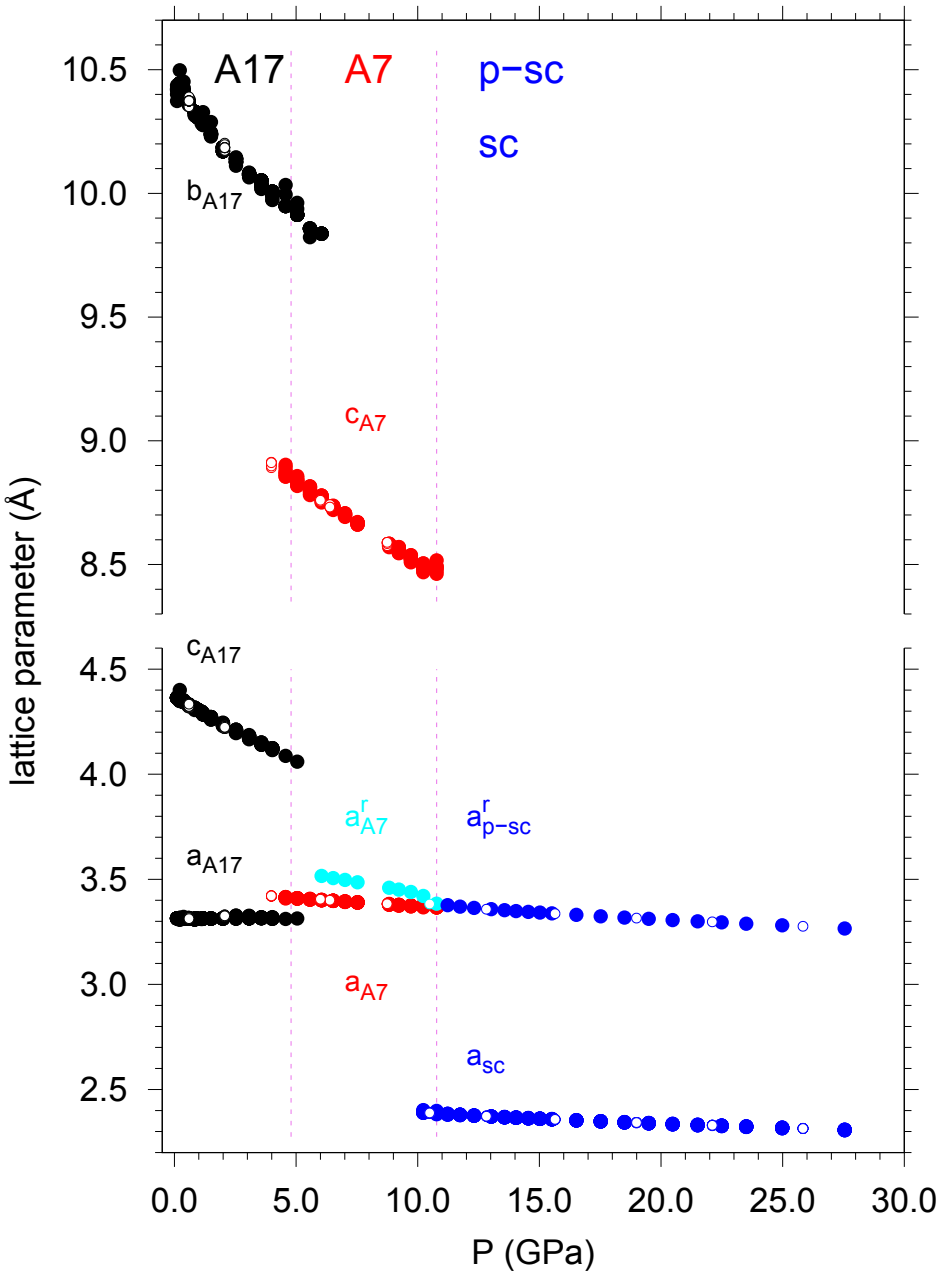

Figure S-1: Room T pressure evolution of the lattice parameters of bP using He as pressure transmitting medium in the orthorhombic A17 (black circles: a_{A17}, b_{A17}, c_{A17}), hexagonal A7 (red circles: a_{A7}, c_{A7}) and rhombohedral p-sc (blue circles: a^r_{p-sc}) structures. For the A7 structure also the pressure evolution of lattice parameter a^r_{A7} (cyan circles), obtained by Rietveld refinement of the data adopting the rhomboehdral cell description ($R\bar{3}m$) as in the case of p-sc, is displayed for comparison with the a^r_{p-sc} values. The a_{sc} data, calculated assuming a sc structure (see text in ESI-5), are reported for comparison with existing literature. Solid and empty circles respectively refer to data acquired during compression and decompression. The vertical dotted lines respectively indicate the A17 to A7 and the A7 to p-sc phase transitions. The ordinate axis has been broken taking care to display the same unit scale for the lattice parameters above and below the break, in order to appreciate the different slope of the pressure evolutions for the lattice parameters.

Table S-1: Parameters of the A7 and p-sc structure obtained adopting a rhombohedral cell description ($R\bar{3}m$) by Rietveld refinement of the XRD patterns, acquired during the compression of bP in the presence of He. As specified by the units, the volume reported in the table is referred to the unit cell, which contains two atoms. The atomic volume is thus obtained by dividing the unit cell volume by 2.

T (K)	P (GPa)	a (Å)	α (degree)	u	U_{iso}	d_1 (Å)	d_2 (Å)	V(Å^3)	wR factor
298	6.05	3.516(5)	57.823(7)	0.2342(2)	0.054(1)	2.292(1)	2.6198(2)	29.2090(13)	0.01152
298	6.525	3.506(5)	57.939(7)	0.2343(2)	0.053(1)	2.288(1)	2.6130(2)	29.0317(13)	0.01152
298	7.01	3.497 (5)	58.037(7)	0.2343(2)	0.052(1)	2.285(1)	2.6071(2)	28.8712(13)	0.01082
298	7.525	3.486(5)	58.148(7)	0.2345(2)	0.056(1)	2.282(1)	2.5986(2)	28.6884(12)	0.01063
298	8.825	3.460(5)	58.446(7)	0.2345(2)	0.059(1)	2.271(1)	2.5835(2)	28.2382(11)	0.00985
298	9.225	3.451(5)	58.538(7)	0.2351(3)	0.060(1)	2.273(1)	2.5719(2)	28.0997(12)	0.01035
298	9.72	3.440(5)	58.676(7)	0.2351(3)	0.059(1)	2.268(1)	2.5658(2)	27.9180(12)	0.01049
298	10.23	3.42(1)	58.96(2)	0.2353(5)	0.056(2)	2.263(2)	2.5540(3)	27.6442(26)	0.01772
298	10.775	3.384(6)	59.667(9)	0.2396(4)	0.065(1)	2.290(2)	2.4909(2)	27.1838(15)	0.01239
298	11.23	3.377(5)	59.716(7)	0.2404(4)	0.066(1)	2.294(2)	2.4777(1)	27.0454(11)	0.01014
298	11.74	3.370(6)	59.744(9)	0.2417(5)	0.083(1)	2.302(2)	2.4605(2)	26.9127(12)	0.01231
298	12.315	3.364(6)	59.767(9)	0.2418(5)	0.085(1)	2.297(2)	2.4560(2)	26.7829(12)	0.01219
298	13.02	3.358(6)	59.787(9)	0.2421(5)	0.089(1)	2.297(2)	2.4483(2)	26.6370(12)	0.01291
298	13.57	3.353(7)	59.80(1)	0.2422(5)	0.093(2)	2.296(2)	2.4433(2)	26.5295(12)	0.01289
298	14.04	3.349(7)	59.80(1)	0.2423(5)	0.093(2)	2.293(2)	2.4406(2)	26.4480(12)	0.01331
298	14.545	3.345(7)	59.81(1)	0.2429(5)	0.098(2)	2.296(2)	2.4319(2)	26.3588(11)	0.01352
298	15.025	3.342(7)	59.81(1)	0.2430(5)	0.099(2)	2.295(2)	2.4279(2)	26.2758(12)	0.01356
298	15.515	3.338(7)	59.81(1)	0.2437(6)	0.010(2)	2.299(3)	2.4186(2)	26.1911(12)	0.01400
298	16.52	3.331(7)	59.82(1)	0.2443(7)	0.096(2)	2.300(3)	2.4069(2)	26.0222(12)	0.01414
298	17.52	3.324(6)	59.815(9)	0.2445(7)	0.095(2)	2.296(3)	2.4005(2)	25.8648(11)	0.01395
298	18.5	3.318(6)	59.803(8)	0.2450(7)	0.089(1)	2.297(3)	2.3906(2)	25.7176(10)	0.01334
298	19.495	3.312(5)	59.800(7)	0.2464(9)	0.088(1)	2.305(4)	2.3728(2)	25.5733(10)	0.01284
298	20.475	3.306(5)	59.795(7)	0.2453(7)	0.086(1)	2.291(3)	2.3787(1)	25.4309(9)	0.01228
298	21.505	3.300(4)	59.783(6)	0.2461(8)	0.082(1)	2.293(4)	2.3673(1)	25.2918(9)	0.01200
298	22.495	3.295(5)	59.784(8)	0.2460(1)	0.079(1)	2.287(4)	2.3663(2)	25.1671(11)	0.01523
298	23.505	3.289(4)	59.791(6)	0.2458(8)	0.077(1)	2.283(3)	2.3619(1)	25.0393(8)	0.01197
298	24.98	3.281(4)	59.801(6)	0.2455(7)	0.073(1)	2.275(3)	2.3593(1)	24.8519(8)	0.01226
298	27.55	3.266(4)	59.830(5)	0.247(1)	0.072(9)	2.283(5)	2.3310(1)	24.5471(7)	0.01188

ESI-6. Equation of state of the A17, A7 and p-sc structures of Phosphorus.

Whereas our *V(P)* values were evaluated for the p-sc structure, all literature data were obtained by assuming a sc structure. Furthermore, whereas our values are limited to the 0-30 GPa pressure range, in which the p-sc structure has been shown to exist,[20] literature data by Akahama *et al.*[14] were obtained across a much larger pressure range extending up to 103 GPa, with only a few points below 30 GPa, thus poorly describing the pressure region where the EOS exhibits its maximum negative slope. Even if the values reported by Kikegawa *et al.*[10] refer to a similar pressure range up to 32 GPa, they are instead affected by a significantly lower precision, as indicated by the larger scattering with respect to our data (Figure 2). Finally, the values reported by Clark *et al.*,[26] besides being more sparse and scattered, were obtained using P_4 as starting material.

Table S-2: Initial volume (V_0), bulk modulus at ambient pressure (B_0) and its pressure derivative (B') at ambient pressure for the A17, A7 and p-sc phases of bP hydrostatically compressed in He (bP/He, this study) and their comparison with literature data from the work of Kikegawa,[10] Akahama[14] and Clark,[26] where non-hydrostatic pressure transmitting media (PTM) were used and the sc structure reported. BM indicates a Birch-Murnaghan equation type.

Exp	PTM	Phase	V_0 (Å^3)	B_0 (GPa)	B'	EOS type
bP/He	He	A17	18.91±0.02	33.3±1.3	3.1±0.6	Vinet
Kikegawa *et al.*[10]	NaCl	A17	18.9±0.6	36±2	4.5±0.5	Murnaghan
Clark *et al.*[26]	MeOH:EtOH:H_2O	A17	18.98±0.08	34.7±0.5	-	BM (II order)
bP/He	He	A7	15.88±0.02	68±2	1.9±0.3	Vinet
Kikegawa *et al.*[10]	NaCl	A7	16.6±0.2	46±4	3.0±0.6	Murnaghan
Clark *et al.*[26]	MeOH:EtOH:H_2O	A7	15.97±0.02	65.0±0.6	-	BM (II order)
bP/He	He	p-sc	15.9±0.2	31.5±6.4	9.7±0.7	Vinet
Kikegawa *et al.*[10]	NaCl	sc	15.2±0.2	95±5	2.1±0.8	Murnaghan
Clark *et al.*[26]	MeOH:EtOH:H_2O	sc	15.33±0.02	72.5±0.3	-	BM (II order)
Akahama *et al.*[14]	no	sc	15.52±0.16	70.7±0.9	4.69±0.1	BM (III order)

Author contributions

D.S., M.C, A.B. and R.B. performed the experiments, analyzed the data and discussed the results. K.D. and M.P. analyzed the data and discussed the results. M.S.R. synthesized bP. A.C. assisted at ESRF-ID27. M.C. conceived the experiment and wrote the article.

References

(1) Liu, H.; Neal, A. T.; Zhu, Z.; Luo, Z.; Xu, X.; Tománek, D.; Ye, P. D. Phosphorene: An Unexplored 2D Semiconductor with a High Hole Mobility. *ACS Nano* **2014**, *8*, 4033–4041.

(2) Li, L.; Yu, Y.; Ye, G. J.; Ge, Q.; Ou, X.; Wu, H.; Feng, D.; Chen, X. H.; Zhang, Y. Black phosphorus field-effect transistors. *Nat. Nanotechnol.* **2014**, *9*, 372–377.

(3) Hultgren, R.; Gingrich, N. S.; Warren, B. E. The Atomic Distribution in Red and Black Phosphorus and the Crystal Structure of Black Phosphorus. *J. Chem. Phys.* **1935**, *3*, 351–355.

(4) Brown, A.; Rundqvist, S. Refinement of the crystal structure of black phosphorus. *Acta Cryst.* **1965**, *19*, 684–685.

(5) Zhu, Z.; Tománek, D. Semiconducting Layered Blue Phosphorus: A Computational Study. *Phys. Rev. Lett.* **2014**, *112*, 176802.

(6) Schusteritsch, G.; Uhrin, M.; Pickard, C. J. Single-Layered Hittorf's Phosphorus: A Wide-Bandgap High Mobility 2D Material. *Nano Lett.* **2016**, *16*, 2975–2980.

(7) Wu, M.; Fu, H.; Zhou, L.; Yao, K.; Zeng, X. C. Nine New Phosphorene Polymorphs with Non-Honeycomb Structures: A Much Extended Family. *Nano Lett.* **2015**, *15*, 3557–3562, PMID: 25844524.

(8) Zhao, T.; He, C. Y.; Ma, S. Y.; Zhang, K. W.; Peng, X. Y.; Xie, G. F.; Zhong, J. X. A new phase of phosphorus: the missed tricycle type red phosphorene. *J. Phys. Condens. Matter* **2015**, *27*, 265301.

(9) Jamieson, J. C. Crystal Structures Adopted by Black Phosphorus at High Pressures. *Science* **1963**, *139*, 1291–1292.

(10) Kikegawa, T.; Iwasaki, H. An X-ray diffraction study of lattice compression and phase transition of crystalline phosphorus. *Acta Crystallogr. B* **1983**, *39*, 158–164.

(11) Kikegawa, T.; Iwasaki, H.; Fujimura, T.; Endo, S.; Akahama, Y.; Akai, T.; Shimomura, O.; Yagi, T.; Akimoto, S.; Shirotani, I. Synchrotron-radiation study of phase transitions in phosphorus at high pressures and temperatures. *J. Appl. Cryst.* **1987**, *20*, 406–410.

(12) Katzke, H.; Tolédano, P. Displacive mechanisms and order-parameter symmetries for the A7-incommensurate-bcc sequences of high-pressure reconstructive phase transitions in Group Va elements. *Phys. Rev. B* **2008**, *77*, 024109.

(13) Marqués, M.; Ackland, G. J.; Lundegaard, L. F.; Falconi, S.; Hejny, C.; McMahon, M. I.; Contreras-García, J.; Hanfland, M. Origin of incommensurate modulations in the high-pressure phosphorus IV phase. *Phys. Rev. B* **2008**, *78*, 054120.

(14) Akahama, Y.; Kobayashi, M.; Kawamura, H. Simple-cubic–simple-hexagonal transition in phosphorus under pressure. *Phys. Rev. B* **1999**, *59*, 8520–8525.

(15) Nishikawa, A.; Niizeki, K.; Shindo, K. Electronic Structure of Phosphorus under High Pressure. *Phys. Status Solidi B* **2001**, *223*, 189–193.

(16) Häussermann, U. High-Pressure Structural Trends of Group 15 Elements: Simple Packed Structures versus Complex Host–Guest Arrangements. *Chem. Eur. J.* **2003**, *9*, 1471–1478.

(17) Akahama, Y.; Kawamura, H.; Carlson, S.; Le Bihan, T.; Häusermann, D. Structural stability and equation of state of simple-hexagonal phosphorus to 280 GPa: Phase transition at 262 GPa. *Phys. Rev. B* **2000**, *61*, 3139–3142.

(18) Ahuja, R. Calculated high pressure crystal structure transformations for phosphorus. *Phys. Status Solidi B* **2003**, *235*, 282–287.

(19) Sugimoto, T.; Akahama, Y.; Fujihisa, H.; Ozawa, Y.; Fukui, H.; Hirao, N.; Ohishi, Y. Identification of superlattice structure *cI*16 in the P-VI phase of phosphorus at 340 GPa and room temperature via x-ray diffraction. *Phys. Rev. B* **2012**, *86*, 024109.

(20) Scelta, D.; Baldassarre, A.; Serrano-Ruiz, M.; Dziubek, K.; Cairns, A. B.; Peruzzini, M.; Bini, R.; Ceppatelli, M. Interlayer Bond Formation in Black Phosphorus at High Pressure. *Angew. Chem. Int. Ed.* **2017**, *56*, 14135–14140.

(21) Nilges, T.; Kersting, M.; Pfeifer, T. A fast low-pressure transport route to large black phosphorus single crystals. *J. Solid State Chem.* **2008**, *181*, 1707 – 1711.

(22) Prescher, C.; Prakapenka, V. B. DIOPTAS: a program for reduction of two-dimensional X-ray diffraction data and data exploration. *High. Press. Res.* **2015**, *35*, 223–230.

(23) Toby, B. H.; Von Dreele, R. B. *GSAS-II*: the genesis of a modern open-source all purpose crystallography software package. *J. Appl. Cryst.* **2013**, *46*, 544–549.

(24) Wojdyr, M. *Fityk*: a general-purpose peak fitting program. *J. Appl. Cryst.* **2010**, *43*, 1126–1128.

(25) Boulfelfel, S. E.; Seifert, G.; Grin, Y.; Leoni, S. Squeezing lone pairs: The *A*17 to *A*7 pressure-induced phase transition in black phosphorus. *Phys. Rev. B* **2012**, *85*, 014110.

(26) Clark, S. M.; Zaug, J. M. Compressibility of cubic white, orthorhombic black, rhombohedral black, and simple cubic black phosphorus. *Phys. Rev. B* **2010**, *82*, 134111.